REKAYASA 22 (2) (2024): 71-83

REKAYASA

Jurnal Penerapan Teknologi dan Pembelajaran

http://journal.unnes.ac.id/journals/rekayasa

Aerodynamic Performance Enhancement of Electric Vehicles Using Selig 1223 Airfoil Wing-Type Spoiler: A Computational Fluid Dynamics Study

Fajar Rizqi Sandi Pratama[1], Aldias Bahatmaka[1*], Muklis Amin[1], Cho Joung Hyung[2]

[1]Department of Mechanical Engineering, Universitas Negeri Semarang, Semarang, Indonesia

[2]Interdisciplinary Program of Marine Design Convergence, Pukyong National University, Busan, South Korea

*Email: aldiasbahatmaka@mail.unnes.ac.id

DOI: https://doi.org/10.15294/rekayasa.v22i2.25166

Abstract

The performance of electric vehicles (EVs) is significantly influenced by aerodynamic forces, which directly affect energy consumption and vehicle stability. One of the main challenges in this regard is the increase in lift and drag forces at higher speeds, which compromises efficiency and handling. This study investigates the impact of a wing type rear spoiler, designed using the Selig 1223 airfoil, on the aerodynamic behavior of EVs. A comparative computational fluid dynamics (CFD) simulation was conducted on two vehicle models: one without a spoiler and another equipped with the Selig 1223 spoiler mounted at a 15° angle of attack. Both models were tested under five speed conditions ranging from 40 to 120 km/h. The simulation results demonstrated a notable improvement in aerodynamic performance. The spoiler produced an average reduction in the lift coefficient (Cl) of approximately 110%, while the drag coefficient (Cd) showed only a slight increase, with the highest recorded rise being 13.3% at 120 km/h. Pressure distribution analysis revealed a substantial increase in static pressure at the rear of the vehicle (Point P3), rising from 37.47 Pa to 660.859 Pa, indicating enhanced downforce. Additionally, streamline and velocity contour plots confirmed improved airflow regulation and reduced turbulence behind the vehicle when the spoiler was installed. These findings indicate that the Selig 1223 airfoil spoiler effectively enhances EV stability and safety with minimal aerodynamic penalties, making it a promising aerodynamic enhancement for future electric vehicle designs.

Keywods: computational fluid dynamics, downforce, spoiler design, streamline, vehicle safety.

INTRODUCTION

Technological advancements in electric vehicles (EVs) are increasingly regarded as a practical solution to the global energy crisis and environmental degradation (Süzen et al., 2021). Although the market is still dominated by internal combustion engine (ICE) vehicles, ongoing technological progress is gradually enabling EVs to take their place (Janicka et al., 2022; Yadlapalli et al., 2022). However, this transition faces several challenges, with energy efficiency being among the most critical. Compared to traditional ICE vehicles, EVs tend to have increased overall weight due to the addition of components such as batteries and reinforced structural frames. This added weight directly affects vehicle performance and driving range particularly from an aerodynamic standpoint (Sivaraj et al., 2018).

As a significant portion of electric energy is expended to overcome air resistance, vehicle aerodynamics plays a vital role in enhancing EV efficiency (Afianto et al., 2022). Aerodynamic drag rises with vehicle speed and accounts for over 65% of total energy consumption at speeds around 100 km/h. B esides drag, lift forces arising from pressure distribution and shear stress imbalances can reduce vehicle stability. Thus, optimizing the aerodynamic properties of EVs is essential to improve both energy efficiency and dynamic stability (Kusaeri & Utomo, 2019; Beigmoradi 2025; Ferraris et al., 2021; Mohammadi et al., 2025).

To address these concerns, many researchers have employed computational fluid dynamics (CFD) simulations to analyze and enhance the aerodynamic performance of EVs. This method enables numerical investigation of airflow around vehicles without the need for costly and time intensive wind tunnel experiments. CFD can predict crucial aerodynamic characteristics such as pressure distribution, drag coefficient (Cd), and lift coefficient (Cl). By simulating various vehicle geometries and appendages, CFD allows for the evaluation and optimization of components like underbody diffusers, body contours, and rear spoilers (Bahatmaka et al., 2023; Bahatmaka & Kim, 2019; Elsayed et al., 2021; Sadat et al., 2022; Xia & Huang, 2024).

Among these aerodynamic enhancements, the application of rear spoilers has gained considerable attention. In particular, wing type rear spoilers have been shown to effectively reduce both drag and lift forces while improving high speed stability. Spoilers are also valued for their cost effectiveness, ease of integration, and potential to improve the aesthetic appeal of vehicles. Adding a rear wing spoiler improves a car's high-speed stability and cornering by increasing negative lift, despite causing higher drag and fuel consumption, thus supporting its use for enhanced safety (Ipilakyaa et al., 2018).

However, while extensive research has examined spoiler effects on ICE vehicles, there is limited work focusing specifically on their influence on EVs.

This research gap is notable given the unique aerodynamic demands of EVs, including altered weight distribution and greater emphasis on energy conservation (Chin & Yuan, 2018; Tousi et al., 2015; Alfianto et al., 2022). Most existing studies rely on spoiler designs optimized for ICE platforms, with little attention to cambered airfoil spoilers designed specifically for EVs. Therefore, this study investigates the aerodynamic effects of a cambered Selig 1223 airfoil spoiler mounted on an electric sedan.

The analysis focuses on how the spoiler affects lift, drag, and pressure distribution, using CFD simulations at multiple driving

speeds. This study compares the aerodynamic performance of EV models with and without the rear spoiler. The chosen spoiler design utilizes the Selig 1223 airfoil profile, selected for its high lift characteristics at a 13° angle of attack, making it suitable for EV applications. CFD simulations are used to evaluate the aerodynamic forces primarily drag and lift generated by airfoil and strip type spoilers on EV model (Kumar, 2017; Rajapaksha et al., 2020). Ultimately, the findings from this study are expected to provide insights into more stable and energy efficient EV designs by optimizing spoiler geometry. Moreover, it seeks to contribute to the limited body of aerodynamic research focusing explicitly on EVs, addressing the gap left by studies that center on ICE vehicle aerodynamics.

METHODS

The initial stages of this study are illustrated in Figure 1, which depicts the workflow conducted using a computational fluid dynamics (CFD) simulation approach. The process began with a comprehensive literature review based on relevant journals and previous studies. In the next step, the vehicle was modeled using computer-aided design (CAD) software and positioned within a user-defined simulation domain. Appropriate boundary conditions were then applied, followed by the specification of airflow velocity settings. The final stage of the CFD simulation produced data outputs in the form of streamline flow patterns, pressure distribution, and velocity contours, which were analyzed to evaluate the aerodynamic performance of the vehicle model.

Previous studies have demonstrated that vehicle body shapes with gently sloping roofs can significantly reduce aerodynamic drag by promoting smoother airflow and minimizing turbulence. According to Connolly et al., (2024), a rounded vehicle body without sharp edges improves energy efficiency by lowering aerodynamic resistance. Wing spoilers are often used in cars to improve aerodynamics by guiding airflow better over the rear, helping reduce lift and drag for greater stability at high speeds.

The Selig 1223 airfoil was selected for this study due to its favorable aerodynamic properties, particularly its relatively low maximum lift coefficient, which makes it suitable for electric vehicle (EV) applications where drag reduction is essential. Arabi & Ilias Inam, (2024) as well as Karthikeyan et al (2024), found that the Selig 1223 airfoil can generate significant downforce without a substantial drag penalty, thus improving vehicle stability at higher speeds. In addition, the angle of attack of a spoiler plays a critical role in balancing downforce and drag. Prior research indicates that an angle of approximately 15° is effective in maximizing downforce while maintaining acceptable drag levels, there by contributing to overall aerodynamic stability. However, despite numerous studies on vehicle aerodynamics and spoiler design, limited research has specifically addressed the use of the Selig 1223 wing type spoiler in the context of electric vehicles especially in optimizing the angle of attack to achieve both high downforce and low drag.

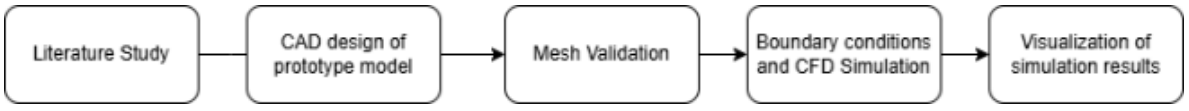

Figure 1. Process stages of CFD simulation

To address this research gap, the present study utilizes computational fluid dynamics (CFD) to analyze the aerodynamic performance of an electric vehicle equipped with a Selig 1223 spoiler set at a 15° angle of attack. The objective is to contribute new insights into spoiler optimization for EVs. To support this investigation, a prototype EV model was developed to examine how the integration of the Selig 1223 spoiler affects airflow, downforce, and drag characteristics under various speed conditions.

MODEL

Based on aerodynamic design principles established in previous literature, a baseline automotive prototype, referred to as Model 1, was developed using the Surface module in SolidWorks. This model was designed to reflect the dimensions of an electric vehicle while aiming to minimize aerodynamic resistance. Figure 2 presents axonometric views of the front and rear perspectives of Model 1. To enhance airflow and reduce turbulence, the design incorporated a gently sloped roofline and smoothly contoured surfaces. These features were selected in accordance with the aerodynamic criteria outlined by Connolly et al., (2024).

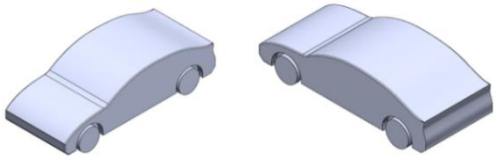

Figure 2. Front and rear axonometric views of Model 1

The dimensional specifications of Model 1, shown in Figure 3, were adjusted to closely resemble a reference vehicle, ensuring that aerodynamic characteristics were maintained throughout the modeling process. To assess the influence of a rear spoiler on aerodynamic performance, a modified version referred to as Model 2 was created by mounting a Selig 1223 wing type spoiler to the rear section of Model 1, as illustrated in Figure 4. The Selig 1223 airfoil was selected due to its favorable aerodynamic characteristics, particularly its ability to generate increased **d**ownforce with minimal drag penalty, as reported in prior studies (Arabi & Ilias Inam, (2024); Karthikeyan et al (2024)).

The dimensional configuration of Model 2, including the spoiler, is shown in Figure 5. The spoiler was positioned at a 15° angle of attack, a setting identified as optimal for increasing downforce and enhancing aerodynamic stability without significantly increasing drag. This configuration facilitated a comparative aerodynamic analysis between the baseline and modified models under consistent simulation parameters.

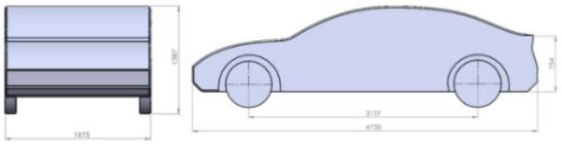

Figure 3. Dimensional illustration of CAD Model 1

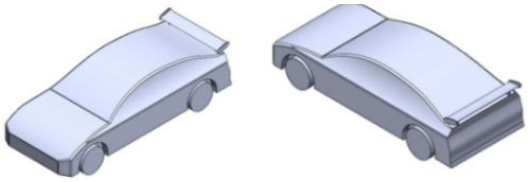

Figure 4. Front and rear axonometric views of Model 2 with Selig 1223 wing-type spoilers

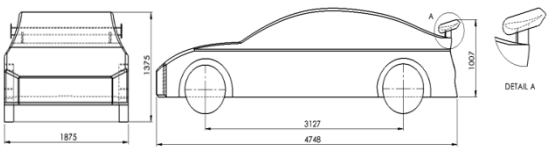

Figure 5. Dimensional illustration of CAD Model 2 and Selig 1223 wing spoiler shape

Mesh Validation

A mesh convergence analysis was conducted in this study to ensure that the computational fluid dynamics (CFD) simulation results were not significantly influenced by the selected mesh resolution (Naik et al., 2019). To achieve this, several mesh configurations with varying element counts were tested, ranging from coarse to fine resolutions. The outcomes of these configurations were compared with reference data from previous research (Scurtu et al., 2020), as shown in Table 1.

Table 1. Simulation results from research (Scurtu et al., 2020)

Velocity (m/s)	Drag Force (N)
14	80.038
25	260.808
34	485.899
55	1276.659

For validation purposes, simulations were carried out at a velocity of 25 m/s using various mesh configurations. This comparison ensured that the selected mesh produced accurate results consistent with the reference data.

As illustrated in Figure 6, the drag force values obtained from different mesh resolutions were plotted against the reference to evaluate convergence behavior. Based on the findings, mesh configuration 2, which contained 466.268 cells, was selected as the optimal setup. It produced a drag force of 260.900 N, with a relative error of only 0.04% compared to the reference. Owing to its high accuracy, this configuration was used for all subsequent CFD simulations.

The computational domain was designed to simulate airflow around the vehicle accurately, with dimensions of 25 m (length), 5 m (width), and 4 m (height) to minimize boundary effects and ensure numerical stability. The vehicle was placed 5 m from the inlet and 15 m from the outlet to allow proper airflow development and wake formation, following the recommendations of Scurtu et al. (2020). To replicate real-world driving conditions, airflow velocities of 40–120 km/h were applied, reflecting typical speed limits commonly encountered on Indonesian roads. A velocity inlet and pressure outlet were defined at the front and rear boundaries, respectively, while no-slip and symmetry conditions were applied to the surrounding surfaces. Additional boundary conditions are summarized in Table 2.

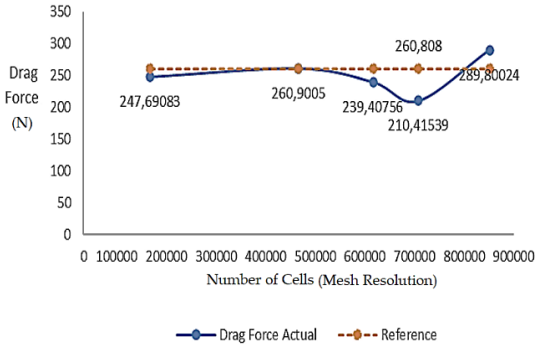

Figure 6. Comparison graph of mesh configuration

CFD Setup and Boundary Conditions

The computational domain used in the CFD simulation is illustrated in Figure 7. To replicate real-world airflow conditions similar to those in a wind tunnel, the vehicle model was positioned within a virtual environment.

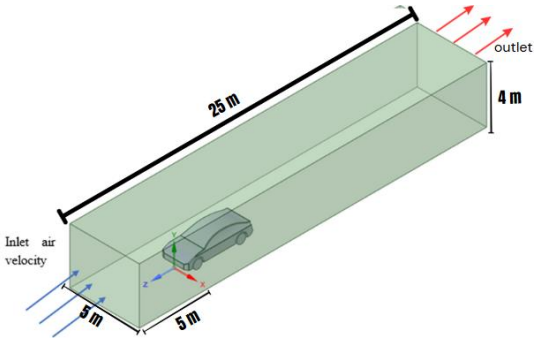

Figure 7. Computational domain in CFD

The domain size was carefully chosen to ensure realistic airflow behavior and to minimize boundary effects that might distort the simulation results.

Table 2. Boundary conditions for CFD Setup

Boundary Condition	Type	Description
Domain	Fluid	25 m (length) x 5 m (width) x 4 m (height)
Material	Fluid	Air (Density: 1.225 kg/m^3)
Viscosity		k-epsilon Realizable (k-ε)
Inlet Boundary	Velocity inlet	V = 40, 60, 80, 100, 120 km/h, perpendicular to the inlet
Outlet Boundary	Pressure outlet	Standard atmospheric pressure
Left, right, and top surface body surface	Wall	No slip wall conditions
Ground	Wall	V = 40, 60, 80, 100, 120 km/h, opposite to the wind speed

The solver algorithm employed a combination of the SIMPLE and Coupled methods, commonly adopted in steady-state flow simulations. Convergence was monitored using residual plots and specific solution variables, including lift, drag, pressure, velocity, and the drag (Cd) and lift (Cl) coefficients. The simulation was considered converged when these variables stabilized to the third or fourth decimal place (Deng et al., 2023; Duc et al., 2023; Džijan et al., 2021; Li et al., 2024; Yudianto et al., 2023).

To ensure numerical accuracy and solution convergence, second-order upwind discretization was used for momentum, turbulent kinetic energy, and dissipation rate equations. Although this method may exhibit slower convergence, it preserves solution stability and precision.

The final outputs obtained from the simulation consisted of the drag coefficient (Cd), lift coefficient (Cl), static pressure contours, as well as streamline and velocity vector plots. These results were utilized to evaluate and compare the aerodynamic performance between the two vehicle configurations one with and one without the integration of the Selig 1223 wing type spoiler.

RESULTS AND DISCUSSION

Filtration Effectiveness in Reducing Heavy Metal Content Streamline

The comparison graphs of drag and lift coefficients between Model 1 and Model 2 across varying speeds are shown in Figure 8(a) and Figure 8(b). The corresponding numerical values for each speed scenario are provided in Table 3, which summarizes the variations in lift coefficient (Cl) and drag coefficient (Cd) for speeds ranging from 40 to 120 km/h.

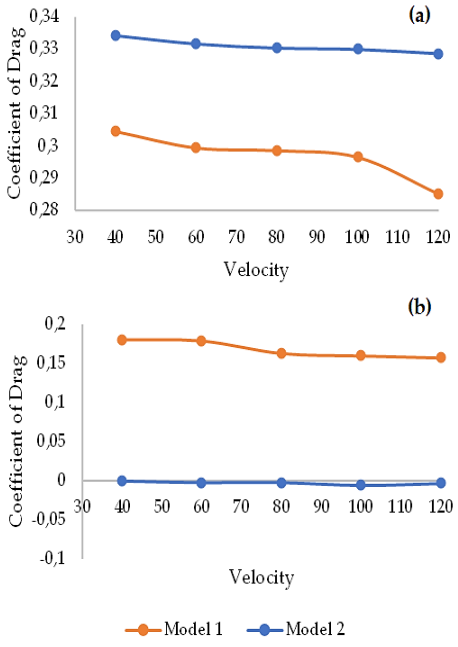

Figure 8. Comparison (a) the graph of drag, (b) the graph of lift for Models 1 and 2

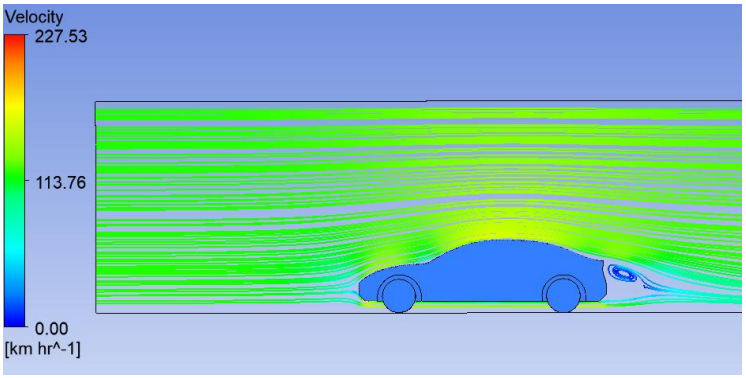

Figure 9. Velocity streamlines of the air passing through Model 1 at 120 km/h.

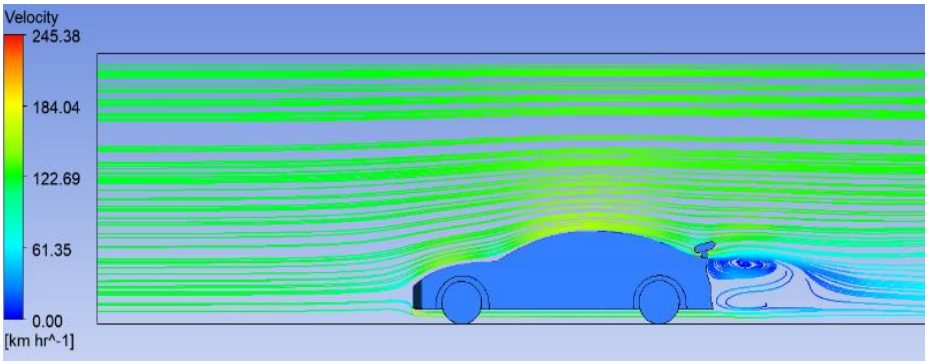

Figure 10. Velocity streamlines of the air passing through Model 2 at 120 km/h

Table 3. Variation of Cl & Cd of each scenario at different speeds

Velocity (km/h)	C_l/C_d	Model 1	Model 2
40	C_l	0,1798	-0,0005
	C_d	0,3046	0,3342
60	C_l	0,1783	-0,0025
	C_d	0,2994	0,3316
80	C_l	0,1622	-0,0025
	C_d	0,2986	0,3304
100	C_l	0,1590	-0,0061
	C_d	0,2965	0,3300
120	C_l	0,1564	-0,0036
	C_d	0,2901	0,3287

It can be observed that for Model 1, which lacks a rear spoiler, the drag coefficient (Cd) consistently decreases as the velocity increases, while the lift coefficient (Cl) remains relatively stable, with a slight decrease at higher speeds. In contrast, Model 2, which is equipped with the Selig 1223 wing type spoiler, exhibits more stable Cl and Cd values across all tested velocities, with only minor fluctuations.

Interestingly, although Model 2 demonstrates improved aerodynamic consistency, its Cl values are negative across all speeds, indicating the generation of downforce. This aerodynamic behavior ensures better road grip and reduces the potential for vehicle instability, especially at high speeds or during sharp maneuvers. These findings are further supported by the streamline velocity plots shown in Figures 9 and 10, which depict the airflow around both vehicle models at 120 km/h.

The visualization in Figure 9 (Model 1) shows a larger wake region behind the vehicle, indicating higher turbulence and lift. In contrast, Figure 10 (Model 2) shows how the airfoil spoiler redirects airflow downward, reducing lift and improving vehicle stability. The spoiler generates reverse lift (i.e., downforce), enhancing traction and control, particularly under high-speed conditions

Pressure

The pressure values at three monitoring points (P1, P2, and P3) for both Model 1 (without spoiler) and Model 2 (with Selig 1223 wing-type spoiler) at speeds ranging from 40 km/h to 120 km/h are presented in Table 4. Figures 11 and 12 visualize the pressure contours at 120 km/h, indicating regions of high and low pressure on each vehicle configuration. From the results, a significant increase in pressure is observed at P2 and especially at P3 for Model 2, confirming the aerodynamic effect of the spoiler. For instance, at 120 km/h, the pressure at P3 reaches 660.859 Pa in Model 2, compared to only 37.47 Pa in Model 1. This increased rear-end pressure is directly associated with the generation of downforce, which enhances vehicle stability during high-speed travel.

The comparison of pressure distributions clearly shows that the presence of a spoiler substantially increases pressure at the rear of the vehicle, particularly at points P2 and P3. This redistribution enhances downforce, improving grip and stability. As shown in Figure 13, the pressure rise at P3 increases with speed, further highlighting the spoiler's growing influence at higher velocities.

In both models, pressure at P1 (the front of the vehicle) also increases with speed. However, Model 2 shows consistently higher values, indicating that the spoiler design contributes to altered pressure fields that reinforce the rear stability of the car.

Table 4. Pressure plot results at 3 points of each scenario at different speeds

Velocity (Km/h)	Pressure (Pa)	Model 1	Model 2
40	P1	76.49	75.22
	P2	23.07	42.35
	P3	3.45	64.3
60	P1	169.709	168.43
	P2	64.57	94.85
	P3	15.33	154.305
80	P1	283.87	297.034
	P2	101.86	172.315
	P3	15.45	283.384
100	P1	395.25	495.338
	P2	194.58	271.541
	P3	43.1	467.909
120	P1	563.409	707.5
	P2	246.08	396.233
	P3	37.47	660.859

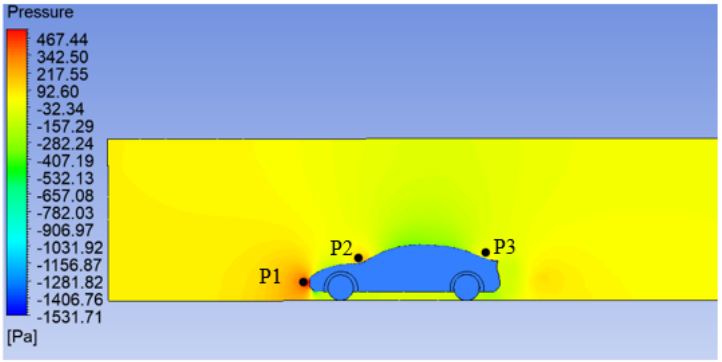

Figure 11. Model 1 pressure contour at 120 km/h speed

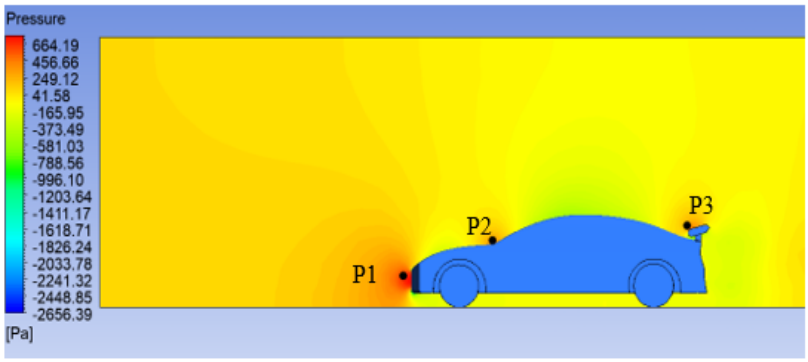

Figure 12. Model 2 pressure contour at 120 km/h speed

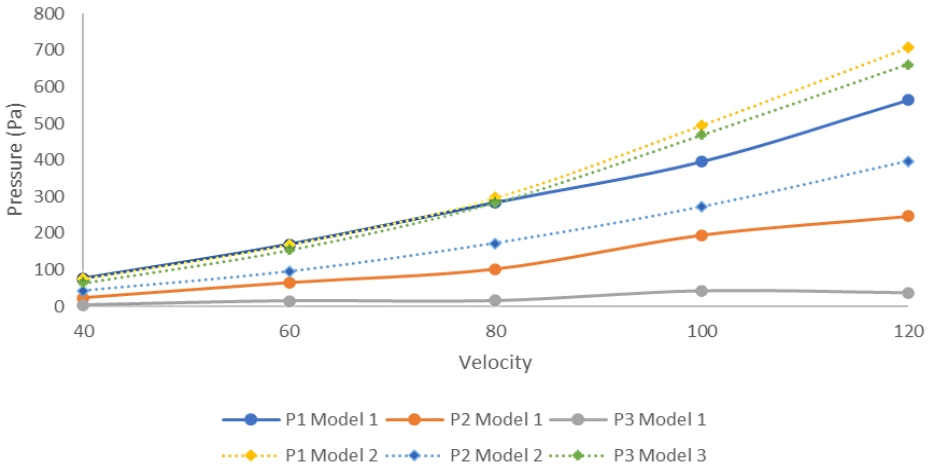

Figure 13. Comparison graph of pressure

Velocity

The velocity contour plots for Models 1 and 2 at 100 km/h are shown in Figures 14 and 15. While the airflow around the front, roof, and lower parts of the car is relatively similar between the two configurations, the flow behavior at the rear differs notably. Model 1 shows more pronounced flow separation and wake turbulence at the back, whereas Model 2 demonstrates more directed airflow due to the presence of the spoiler, resulting in improved aerodynamic efficiency.

These airflow differences at the rear are further visualized in Figure 16, which compares the streamline patterns between the two models. The spoiler in Model 2 helps direct the airflow downward, reducing rear-end lift and increasing downforce. However, this advantage comes with the cost of slightly increased turbulence behind the vehicle. In contrast, Model 1 exhibits minimal downforce generation and more dispersed airflow, which contributes to lower stability and greater wake formation.

The addition of a Selig 1223 airfoil wing-type spoiler enhances aerodynamic stability by increasing rear-end pressure and downforce. Although it introduces additional turbulence at the vehicle's rear, the overall effect favors improved handling and stability, especially at high speeds or during sudden maneuvers. Therefore, by increasing downforce, an airfoil wing spoiler can significantly boost vehicle stability; however, this comes at the expense of more pronounced turbulence at the back of the vehicle.

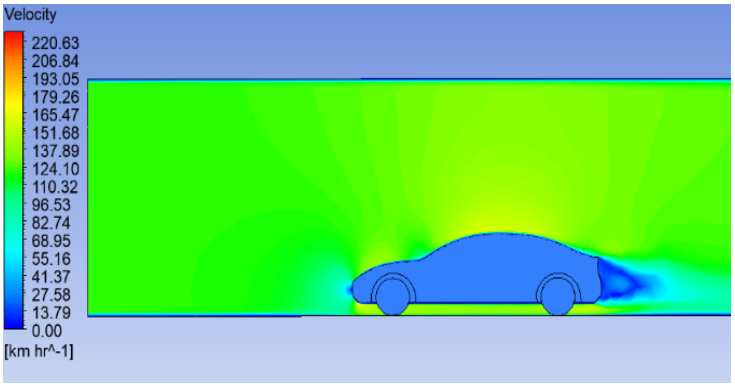

Figure 14. Velocity contours of airflow passing through Model 1 at 100 km/h.

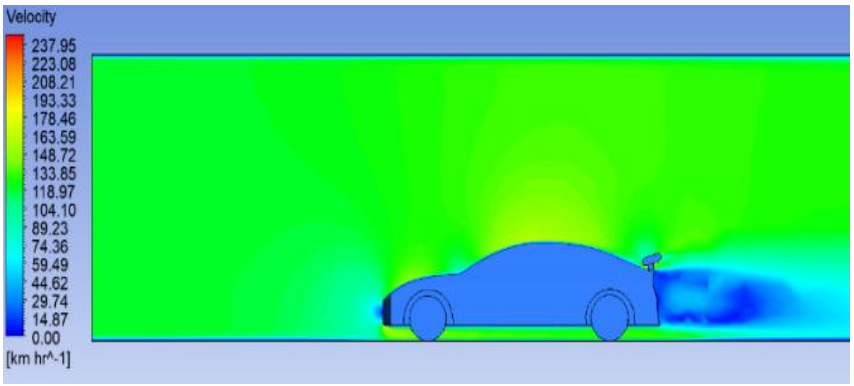

Figure 15. Velocity contours of airflow passing through Model 2 at 100 km/h.

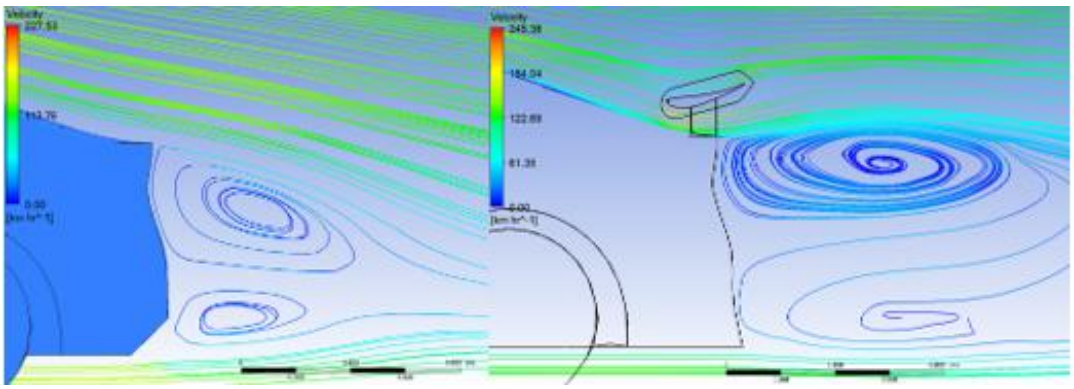

Figure 16. Differences in streamlining passing Model 1 and Model 2 at the rear of the vehicle

CONCLUSION

Simulation results show that applying a Selig 1223 airfoil spoiler significantly improves the aerodynamic performance of electric vehicles (EVs). The spoiler reduced lift by around 110%, enhancing stability at high speeds, while the drag increase remained minimal at 13.3% for 120 km/h. The spoiler also increased rear pressure, generating downforce up to 660.859 Pa, which improves traction and overall vehicle control. Flow visualization confirmed that the airfoil effectively reduces turbulence, regulates airflow, and optimizes streamline direction, especially at a 15° angle of attack. This study introduces the application of a cambered airfoil on an EV platform, offering new insights beyond conventional flat spoiler designs commonly used on internal combustion engine (ICE) vehicles. Future work should explore advanced spoiler geometries,

active aerodynamic systems, and validate these findings through experimental testing under controlled and real-world conditions.

ACKNOWLEDGMENT

The authors would like to thank Universitas Negeri Semarang for providing financial assistance for this research and the Department of Engineering at Universitas Negeri Semarang for supplying the necessary resources and facilities. Special thanks are extended to Dr. Eng. Aldias Bahatmaka for his valuable guidance throughout this study and to Muklis Amin for his contributions to the research.

REEFERENCES

Afianto, D., Han, Y., Yan, P., Yang, Y., Elbarghthi, A. F., & Wen, C. (2022). Optimisation and efficiency improvement of electric vehicles using computational fluid dynamics modelling. *Entropy*, *24*(11), 1584.

Arabi, M. A., & Ilias Inam, M. (2024). Aerodynamic Characteristics of an FSAE Car Rear Wing with Multi-Element S1223 Airfoil. *SSRN Electronic Journal*, *December*, 1–6.

Bahatmaka, A., & Kim, D. J. (2019). Numerical approach for the traditional fishing vessel analysis of resistance by cfd. *Journal of Engineering Science and Technology*, *14*(1), 207–217.

Bahatmaka, A., Wibowo, M. Y., Ghyfery, A. A., Harits, M., Anis, S., Fitriyana, D. F., Naryanto, R. F., Setiyawan, A., Setiadi, R., Prabowo, A. R., & others. (2023). Numerical Approach of Fishing Vessel Hull Form to Measure Resistance Profile and Wave Pattern of Mono-Hull Design. *Journal of Advanced Research in Fluid Mechanics and Thermal Sciences*, *104*(1), 1–11.

Beigmoradi, S. (2025). Harmonizing aerodynamic efficiency, stability, and acoustic excellence: multi-objective optimization for electric vehicle rear-end design. *Multiscale and Multidisciplinary Modeling, Experiments and Design*, *8*(1), 56.

Chin, K. Y., Cheng, S. Y., & Mansor, S. (2018). Yaw angle effect on the aerodynamic performance of hatchback vehicle fitted with combo-type spoiler. *Proceedings of Mechanical Engineering Research Day 2018*, *2018*, 69-70.

Connolly, M. G., Ivankovic, A., & O'Rourke, M. J. (2024). Drag reduction technology and devices for road vehicles - A comprehensive review. *Heliyon*, *10*(13), e33757.

Deng, Y., Lu, K., Liu, T., Wang, X., Shen, H., & Gong, J. (2023). Numerical Simulation of Aerodynamic Characteristics of Electric Vehicles with Battery Packs Mounted on Chassis. *World Electric Vehicle Journal*, *14*(8), 216.

Duc, T. D., Pham, D., Vinh, X., & Duy, N. (2023). *Aerodynamics Simulation of Prototype Car Based on CFD Technology*. 1–13.

Džijan, I., Pašić, A., Buljac, A., & Kozmar, H. (2021). Aerodynamic characteristics of two slipstreaming race cars. *Journal of Mechanical Science and Technology*, *35*(1), 179–186.

Elsayed, O., Omar, A., Jeddi, A., Elhessni, S., & Hachimy, F. Z. (2021). Drag Reduction by Application of Different Shape Designs in a Sport Utility Vehicle. *International Journal of Automotive and Mechanical Engineering*, *18*(3), 8870–8881.

Ferraris, A., De Cupis, D., de Carvalho Pinheiro, H., Messana, A., Sisca, L., Airale, A. G., & Carello, M. (2021). *Integrated design and control of active aerodynamic features for high performance electric vehicles* (No. 2020-36-0079). SAE Technical Paper.

Ipilakyaa, T. D., Tuleun, L. T., & Kekung, M. O. (2018). Computational fluid dynamics modelling of an aerodynamic rear

spoiler on cars. *Nigerian Journal of Technology*, *37*(4), 975-980.

Janicka, A., Zawiślak, M., Głogoza, A., & Włostowski, R. (2022). Optimization of the electric bus radiator design in terms of noise emissions and energy consumption by computational fluid dynamics. *Combustion Engines*, *191*(4), 41–50.

Karthikeyan, P. N., & Radhakrishnan, J. (2024). *Optimizing High-Lift Airfoils for Formula Student Vehicles* (No. 2024-01-5059). SAE Technical Paper.

Kumar, D. M. V. S. (2017). Design, Analysis and Manufacturing of a Car Rear Spoiler for Drag Reduction. *Iarjset*, *4*(6), 89–96.

Kusaeri, D., & Utomo, M. (2019). *Analysis of Aerodynamics Urban Electric Car Using Computational Fluid Dynamics*. *203*(Iclick 2018), 40–43.

Mohammadi, M., Nazemosadat, S. M. R., Fazel, D., & Lari, Y. B. (2025). An integrated approach for structural modeling, modal analysis, and aerodynamic evaluation of an electric vehicle body shell using finite element method and computational fluid dynamics. *Materials Today Communications*, *45*, 112331.

Naik, N., Shenoy, P., Nayak, N., Awasthi, S., & Samant, R. (2019). Mesh convergence test for finite element method on high pressure gas turbine disk rim using energy norm: An alternate approach. *International Journal of Mechanical Engineering and Technology*, *1*, 765–775.

Li, J., Liu, F., & Wang, L. (2024). Design and Aerodynamic Characteristics Analysis of an Electric Racecar Body Based on CFD. *World Electric Vehicle Journal*, *15*(5).

Rajapaksha, R. G. S. K., Kurukulasooriya, K. D. P. C., Herath, H. M. T. M., Rangajeeva, S. L. M. D., & Bandara, R. M. P. S. (2020). Aerodynamic Analysis of Rear Wings and Rear Spoilers of Passenger Automobiles. *Annual Sessions of IESL*, *October 2018*, 515–522.

Sadat, M., Albab, N., Chowdhury, F., & Khan, M. M. A. (2022). Numerical Simulation Approach to Investigate the Effects of External Modifications in Reducing Aerodynamic Drag on Passenger Vehicles. *International Journal of Automotive and Mechanical Engineering*, *19*(1), 9563–9576.

Scurtu, L., Jurco, A., Borza, E. V., Mariasiu, F., Vlad, N., & Morariu, S. (2020). Aerodynamic Study of an Electric Vehicle Prototype. *The 30th SIAR International Congress of Automotive and Transport Engineering*, *1*, 485–493.

Sivaraj, G., Parammasivam, K. M., & Suganya, G. (2018). Reduction of aerodynamic drag force for reducing fuel consumption in road vehicle using basebleed. *Journal of Applied Fluid Mechanics*, *11*(6), 1489–1495.

Sudin, M. N., Abdullah, M. A., Shamsuddin, S. A., Ramli, F. R., & Tahir, M. M. (2014). Review of research on vehicles aerodynamic drag reduction methods. *International Journal of Mechanical and Mechatronics Engineering*, *14*(2), 35–47.

Süzen, Y. O., Özdoğan, E., San, İ., Gürbüz, B., Kaçar, M., Demir, N., & Kaya, M. F. (2021). Cfd Modelling of Voltacar Electric Vehicle Body for the Most Efficient Driving Conditions. *Energy, Environment & Storage*, *1*(3), 34–40.

Tousi, S. M. R., Bayat, P., & Bayat, P. (2015). *Evaluating the Importance of Rear Spoiler on Energy Efficiency of Electri Vehicles*. *5*(4).

Xia, Z., & Huang, M. (2024). Optimizing the Aerodynamic Efficiency of Electric Vehicles via Streamlined Design: A Computational Fluid Dynamics Approach. *International Journal of Heat and Technology*, *42*(3), 865–876.

Yadlapalli, R. T., Kotapati, A., Kandipati, R., & Koritala, C. S. (2022). A review on energy efficient technologies for electric vehicle

applications. *Journal of Energy Storage*, *50*(January), 104212.

Yudianto, A., Solikin, M., Sutiman, S., Arifin, Z., Adiyasa, I. W., & Yudantoko, A. (2023). Aerodynamic investigation of extremely efficient vehicles under side wind conditions. *Revista Facultad de Ingenieria*, *109*, 79–88.